CIRP Annals - Manufacturing Technology 73 (2024) 449–452

Contents lists available at ScienceDirect

CIRP Annals - Manufacturing Technology

journal homepage: https://www.editorialmanager.com/CIRP/default.aspx

Reducing rubber-plastic friction in syringes through microstructured surface design and manufacturing

Marco Sorgato, Kristal Bornillo, Giovanni Lucchetta (2)*

Department of Industrial Engineering, University of Padova, via Venezia 1, Padova 35131, Italy

ARTICLE INFO

Article history:
Available online 4 May 2024

Keywords:
Friction
Micro structure
Injection molding

ABSTRACT

Plastic syringes often rely on silicone oil lubrication to reduce plunger-barrel friction, leading to potential issues like oil droplet release and drug aggregation. This study explored an alternative approach combining two-photon polymerization, laser machining, and microinjection molding to manufacture micro-dimpled structures for low friction. Plastic microdimples with high area density and low aspect ratio significantly reduced the coefficient of friction against rubber, while the dimple profile proved crucial in facilitating replication and demolding. The results of this study provide valuable insights into reducing friction between rubber and plastic, particularly in applications like syringes.

1. Introduction

Prefilled syringes have been increasingly used as alternatives to vial packaging for parenteral drug delivery due to their easy administration, accurate dosing, and reduced contamination. Most commercially available syringes rely on the siliconization of the inner surface barrel to allow for the plunger to move with less force and glide more smoothly. However, silicone oil (SO) droplets have been found in the vitreous of patients after intravitreal injections [1]. Additionally, contaminations of therapeutic protein formulations with silicone oil have caused aggregation, as reported in several cases [2]. The presence of aggregates affects the quality and efficacy of the drugs and can also lead to immunogenicity.

In recent years, silicone oil-free (SOF) syringes that use novel proprietary coating techniques for plunger stoppers have been developed and are currently available in the market [3]. Still, both SOF and siliconized syringes involve a two-step manufacturing process: fabricating the plunger stopper and barrel and then coating with a smooth, uniform, low-friction layer.

One way to reduce friction without altering the surface compositional change and the use of coating is surface texturing. Over the years, many studies have focused on creating optimized textures, particularly in submicron to micron size, to improve tribological performance. There is no total agreement on how the textured surface parameters affect friction, as some surface textures can also increase it [4]. Researchers began to explore the effects of area density, aspect ratio, surface shape, bottom shape profiles, sliding velocity, load applied, and lubrication, among others, on microdimples [5–7]. However, there are still discrepancies in the geometric factors' reported significance and optimal friction reduction values [8]. This is attributable to the variances in the material used, experimental setup, and the geometric dimensional inaccuracies closely related to the processing technology of the surface textures.

Brinksmeier et al., identified that manufacturing processes for textured surfaces, such as milling, turning, and laser machining, produce textures ranging from nano- to millimeter scale [9]. However, their precision can be inconsistent, underscoring the need for high-precision techniques in prototyping. Additionally, for commercial application, it's essential to replicate these functional microstructures through industrial methods like injection molding. Previous research indicates that microstructure characteristics significantly influence the replication quality, as they involve filling the macro cavity that acts as the substrate and the microfeatures, which are difficult to replicate [10]. In addition, the presence of micro features can be challenging during demolding, especially for micro features that are supposed to be on the inside wall of long and hollow core parts, such as syringes: the sliding along the length of the core tool can affect the integrity and functionality of the microfeatures. Hence, it is important to focus not only on the functionality of microstructures but also on their manufacturability and replication for industrial use. Therefore, this paper focuses on studying the effect of surface microdimple geometrical parameters on both functionality, i.e., friction reduction against rubber, and manufacturability intended for syringe applications. Two-photon polymerization (TPP), a high-resolution additive manufacturing technique, was utilized to fabricate prototype samples for factors screening on friction reduction and minimize the variations caused by dimension inaccuracies. The negative shape of the low-friction micro-dimpled structures was then laser ablated on a microinjection molding (μIM) mold and replicated on plastic for the functionality tests.

2. Materials and methods

2.1. TPP prototyping of micro-dimpled structures

The effect on friction reduction of the microdimple geometrical parameters was studied by employing a design of experiments (DoE) approach. A four-factor full factorial design was carried out to screen the effects of microdimple surface shape, bottom profile, aspect ratio,

* Corresponding author.
E-mail address: giovanni.lucchetta@unipd.it (G. Lucchetta).

https://doi.org/10.1016/j.cirp.2024.04.096

Table 1
Geometrical factors settings for the DoE plan.

Factors	Low	High
Surface Shape	Circle	Square
Profile	Flat	Curved or Sloped
Aspect Ratio	0.05	0.5
Area Density (%)	5	50

and area density as factors. The range values for each factor are reported in Table 1. These values were defined considering the literature and replicability using µIM. The width was fixed at 100 µm, based on previous studies. Aspect ratios were derived from the literature's 5 to 50 µm depth range. Area density values were from previous research; 5 to 50 % were used to study friction variation. The simplest shapes were square and circle, with flat or curved/inclined bottom shapes. The inclined profile was of interest, especially for the replication using µIM.

The sample names were abbreviated in this study as 'surface shape and profile' - 'aspect ratio' - 'area density': CF-0.05–50 % stands for a sample with microdimples with a circular surface shape and a flat profile (CF), a 0.05 aspect ratio, and 50 % area density). All widths and diameters were set at 100 µm. The curvature radii for the curved profiles were 2 µm and 50 µm for the 0.05 and the 0.5 aspect ratios, respectively.

The micro-dimpled samples were prototyped using an ultrafine maskless TPP 3D laser lithography machine (Nanoscribe GmbH, Photonic Professional GT). The laser light source has a wavelength of 780 nm, a pulse width of 150 fs, a frequency of 40 MHz to 100 MHz, and a maximum power of 45 mW. The objective used has a 25× magnification. The samples were printed as $4 \times 10 \times 0.2$ mm^3 rectangular substrates with micro-dimpled surfaces from an acrylate-based photoresist, IP-S (Nanoscribe GmbH), on an indium tin oxide-coated glass substrate. After printing, the unpolymerized resin was removed by soaking the sample in propylene glycol monomethyl ether acetate for 30 min and soaking it with isopropyl alcohol for 3 min afterward. The samples were air-dried at ambient temperature and then subjected to a 10-minute UV treatment to ensure complete polymerization.

2.2. Microinjection molding experiments

The molded samples were designed to be a hollow truncated pyramid with the microdimples replicated on two opposite drafted inner walls, shaded red in Fig. 1. It was of interest to know how the microstructures and the draft angle (α) affect the replication and the demoldability of the microtextured part. Hence, a two-factor experiment was conducted. The range values of these factors are reported in Table 2. These settings were based on the results from the previous experiments, and the draft angles were set within the usual range of syringe, i.e., 0.25° to 1° A modular mold tool was used to mount the core inserts and change the microstructure and draft angle. The molded polymer was a

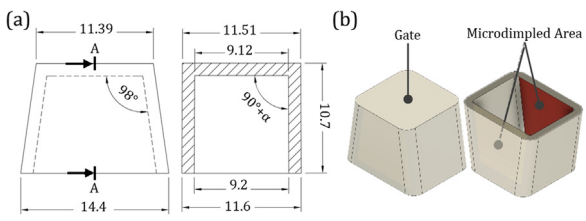

Fig. 1. Molded sample (a) design and dimensions (in millimeters) and (b) location of the gate and micro-dimpled area.

Table 2
Geometrical factors settings for the µIM experiments.

Factors	Settings		
Microtexture shape and profile	Square-Sloped (SS-0.05–50 %)	Circle-Flat (CF-0.05–50 %)	Untextured
Draft angle, α	0.25°	1°	

cyclic olefin copolymer (TOPAS, COC 5013L-10), widely used in biomedical devices due to its high clarity and biocompatibility.

A femtosecond laser (Amplitude, Satsuma HP^2) with a pulse duration of 300 fs and wavelength of 1030 nm was used to fabricate the micropillars (i.e., the negative shape of microdimples) on the surface of the 16MnCr5 steel alloy mold inserts. The laser power was 7 W with a scanning speed of 1080 mm/s. In addition to the four laser-ablated mold inserts, two smooth-surface inserts ($Sa < 0.02$ µm) with varied draft angles were prepared as reference.

The microdimples were replicated on the COC samples using a µIM machine (Wittmann Battenfeld, MicroPower 15). The mold was heated to 100 °C. The flow rate and the holding pressure were set at 2.5 cm^3/s and 170 bar for 5 s respectively.

The ejection force and work, defined as the peak force for pushing the molded part during demolding and the area under the acquired force-time curve, were measured for each molded part using a Kistler 9223A piezoelectric force transducer mounted behind the ejector plate. Twenty molding cycles were conducted to stabilize the µIM process and force monitoring setup. Upon stabilization, the ejection force profiles of the succeeding ten molding cycles were acquired at 1.25 kHz.

2.3. Surface characterization

The surface roughness and microtexture dimensions of the TPP-printed samples, mold inserts, and the replicated surfaces were analyzed using a confocal microscope (Sensofar Neox) at 20× magnification. Height maps of area 877 × 660 µm^2 were extracted and leveled by subtracting the mean plane. The arithmetical mean height (Sa) of the reference and contact surface of the samples was calculated from the S-L surface according to ISO 25,178–2:2021, with an S-filter of 2.5 µm and an L-filter of 80 µm. For TPP-printed samples, four microdimples from each corner and the center part of the sample were chosen for measurement. This sums to a total of 20 measured microdimples per sample. To evaluate the replication and integrity of the microdimples after demolding, five microstructures from each of the nine chosen sites (four corners and five sites on the centerline) were measured for both the inserts and the molded part. This sums up to 45 dimples measured and averaged for each sample. In addition to the confocal microscope, the laser-textured mold inserts were qualitatively observed using a digital microscope (Keyence, VHX-7000).

Friction tests used an RTEC Instruments MFT 5000 tribometer with a 5 N load. Prior, samples and rubbers were washed with isopropyl alcohol and deionized water in an ultrasonic bath for 3 min. A volume of 40 µL of 0.9 % NaCl saline was applied for lubrication. Friction coefficients were obtained by sliding the samples against a 10 mm base diameter conical butyl rubber at 1.33 mm/s. Each sample produced by TPP printing and injection molding was subjected to at least three replication tests.

3. Results

3.1. Characterization of TPP-printed micro-dimpled samples

Fig. 2 shows the surface height maps of the micro-dimpled samples printed using TPP. The top surface of the samples and the reference have $Sa < 150$ nm. The print accuracy was supported by the measured average diameter and width, aspect ratio, and area density

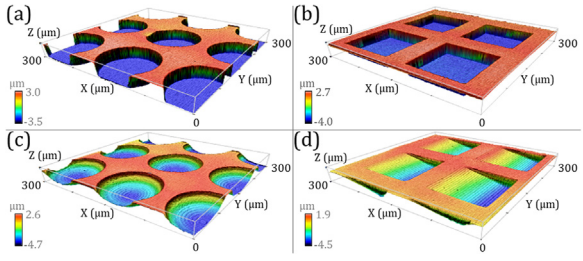

Fig. 2. Height maps of (a) CF,(b) SF,(c) CC, and (d) SS at 0.05 aspect ratio and 50 % area density.

Table 3
Measured average dimensions and standard deviations (s) of the TPP-printed microdimples. Max s is the highest s among all samples for each dimension.

Dimension	Average Values	
Diameter or Width	100.3 µm, max s = 0.5 µm	
Aspect Ratio	0.05; max s = 0.001	0.5; max s = 0.009
Area Density,%	5; max s = 0.11	50; max s = 1.2

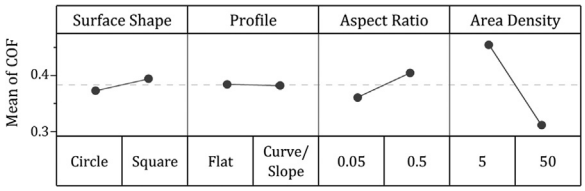

Fig. 3. Main effect plots for COF.

of the samples with low maximum standard deviation within each dimension (Table 3).

The area density had the most significant effect on friction (p-value < 0.001). The main effect of increasing the area density from 5 % to 50 % was to reduce the dynamic coefficient of friction (COF) by 36 %, as shown in Fig. 3. Increasing the surface density of the microstructures on a given surface area decreases the real contact area between the microtextured surface and the opposite sliding surface, reducing the friction between the sliding surfaces [11]. As the area density markedly outweighed the other factors in these experiments, the results were revisited with the area density maintained at its highest level to analyze the secondary effect of the other factors. This approach allowed for determining that only the aspect ratio significantly influences COF among the remaining factors, i.e., surface shape and profile. Increasing the aspect ratio from 0.05 to 0.5, COF increased by 35 %. Microdimples with higher aspect ratios require a larger volume of lubricant to be filled, which is necessary to exert beneficial hydrodynamic pressure that can reduce friction. As the depth of the microdimples increases, it becomes progressively challenging for the lubricant to enter in sufficient volume. The optimal aspect ratio varies in existing literature due to different materials and experimental methods. This study's findings on the optimal aspect ratio fall within the previously reported effective range of 0.1 to 0.02 [8].

3.2. Microinjection-molded micro-dimpled parts

Optimal settings from TPP-printed micro-dimpled sample tests were used to design the µIM samples, focusing on varying dimple shapes and profiles to study their impact on microtexture replication and friction during demolding. Circular dimples with flat profiles and square dimples with sloped profiles were replicated using µIM to assess their manufacturability.

As shown in Fig. 4., micropillars with a 0.05 aspect ratio were successfully fabricated on the surface of the mold inserts by laser

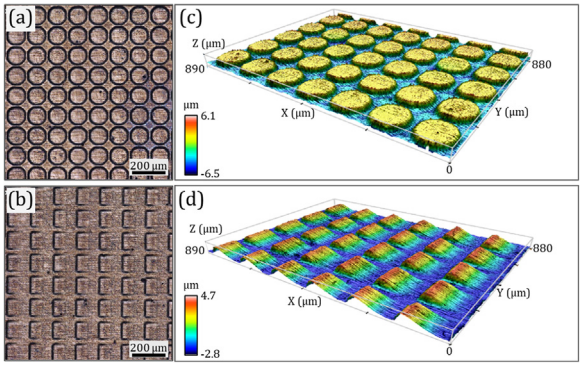

Fig. 4. Digital microscope images of the mold inserts at 500× magnification with cylindrical (a) and square sloped (b) pillar structures, and their corresponding height maps (c) and (d).

Table 4
Measured dimensions of the micropillars on the laser-ablated inserts.

Draft Angle	Shape	Depth (μm)	Area Density (%)	Aspect Ratio
1°	Square	4.95±0.11	51.4 ± 0.89	0.049±8E-4
	Circle	5.12±0.08	50.1 ± 1.06	0.051±5E-4
0.25°	Square	5.03±0.16	51.6 ± 1.24	0.049±1E-3
	Circle	5.10±0.12	50.3 ± 1.74	0.052±2E-3

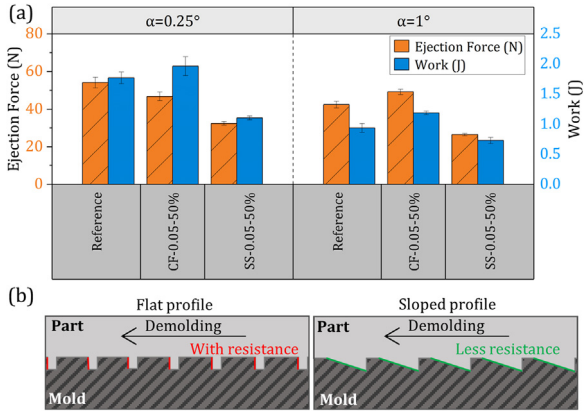

Fig. 5. Measured ejection force and work during demolding of samples with varying draft angles and geometry (a) and illustrations on how the microdimple profiles affect the ejection (b). The error bars represent the standard deviation.

ablation. The optical microscope images suggest that the microstructures were uniformly distributed on the surface. Table 4 summarizes the measured dimensions of the laser-textured micropillars.

Fig. 5a shows the ejection force and work measured during the demolding of the replicated plastic parts. Microstructures on the surface influenced the ejection force regardless of the draft angle. This was most notable in the case of the dimples with a sloped profile, wherein the ejection force was reduced by 39 % relative to the smooth surface reference.

Fig. 5b shows how the inclined profile facilitated an easier sliding motion as no structure hindered its motion. Thus, less force was needed to initiate separation and effectively eject the part from the mold. However, this was not the case for the circular dimples with flat profiles, which only had a 0.6 % reduction in ejection force relative to the reference. The structures served as undercuts on the surface of the plastic part. Hence, when demolding along the core axis, there was resistance due to a mechanical interlocking between the part and the tool surface, which resulted in a higher force needed to initiate the sliding of the solidified polymer over the core tool surface and, thus, a high peak ejection force [12].

It was previously proposed that the ejection force is a function of both adhesion and friction between the plastic part and the mold tool [13]. Increasing the draft angle on a part's walls reduces friction and contact with the mold during demolding, easing ejection. In fact, when the draft angle was increased from 0.25° to 1°, the average work and ejection force were reduced by 41 % and 11.5 %, respectively. As expected, the draft angle had less effect on the ejection force, which strongly depends on the mechanical interlocking. In fact, this is especially evident for the microtextured surfaces. Increasing the draft angle significantly reduces the work needed to slide the part out of the tool continuously because it helps prevent the development of a vacuum between the part and the mold core, thus facilitating smoother removal of the part.

The molded parts were also characterized for the replication quality and integrity of the microdimples. Fig. 6a shows the replication degree of the microdimples with respect to the insert textures at nine different zones of the plastic part surface (Fig. 6b). Sample images of height maps of both circular and square samples in Fig. 6c show that there was no observable damage/deformation caused by demolding along the X-axis. Instead, low ridge height was observed in the X and Y directions for the circular microdimples, and a uniform

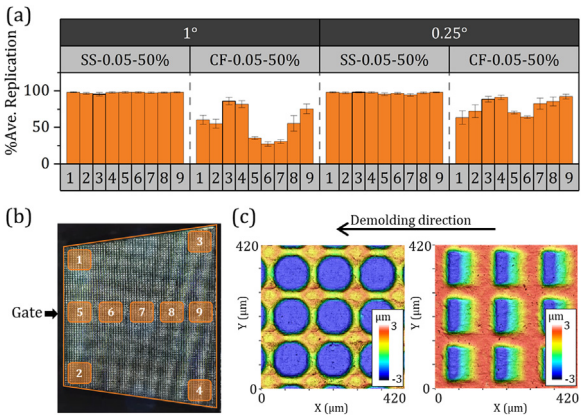

Fig. 6. Microdimples replication degree at varying draft angles and shapes measured at nine zones in the plastic part (b), and the surface map of the replicated parts with circle and square microdimples (c). All dimensions are expressed in micrometers.

surface was observed in the square sample. This implies that the microstructures had preserved their integrity after demolding. The low depth of the circular dimples (Fig. 6a) was due to the hesitation effect during mold filling, which is caused by the thinner pillar-to-pillar distance (25 µm) of the circular dimple as compared to the 40 µm pillar-to-pillar distance of the square dimples. The hesitation effect in µIM refers to a transient phenomenon where the flow of molten polymer temporarily pauses and solidifies as it enters the smallest microfeatures of the mold, thereby hindering their complete replication [14]. This was further supported by the observed higher replication degree at the larger inter-dimple regions where thin ridges intersect (colored orange in the height map of circular dimples). The polymer melt could flow well in these larger areas, thus resulting in better replication. Despite having less effect on the surface functionality, the dimple profile factor played a significant role in microtexture replication.

After molding, the samples were cut in half to expose the microtextured surface for friction test. The COF reduction of the molded samples was compared to the TPP-printed samples of the same geometry, and the results are shown in Fig. 7. The performance of the well-replicated SS-0.05–50 % was comparable to its TPP-printed counterpart, with a negligible difference of 3 %. On the other hand, the CF-0.05–50 % was 32 % less effective compared to its TPP-printed counterpart. The deviation is due to the difference in roughness of the TPP-printed CF-0.05–50 % and its injection-molded counterpart. This resulted from the incomplete replication of the CF microdimples, which increased the *Sa* from 0.26±0.01 µm (mold insert) to 0.35± 0.03 µm (molded part). This was a 225 % increase compared to the *Sa* of the TPP-printed sample. Moreover, the average aspect ratio of the injection-molded CF-0.05–50 % was 0.039±0.08 which was 33 % lower than the aspect ratio of the TPP-printed sample. As for the injection-molded SS-0.05–50 %, the difference with the TPP-printed was an increase in *Sa* by 30 %, and the average aspect ratio by 2 %.

Although the shape and profile of microdimples did not directly influence friction reduction, they significantly impacted it indirectly by playing a crucial role in the replication of microtextures, which, in turn, substantially affects the reduction of friction in molded samples.

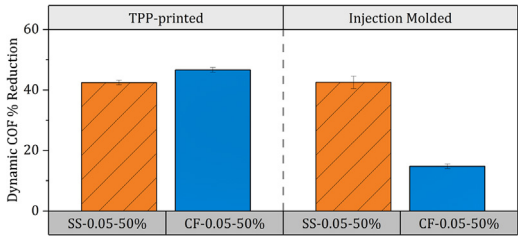

Fig. 7. Comparison of the COF reduction of the same microdimples manufactured using TPP and µIM. The error bars represent the standard deviation.

4. Conclusion

This study assessed how surface microdimple geometries affect syringe functionality and manufacturability. Findings highlighted the significant role of microdimple area density and aspect ratio in friction reduction. Micro injection molding experiments showed the impact of microstructure shape and profile on manufacturability, with squared, sloped microdimples achieving better replication and lower ejection forces, offering insights into friction reduction between rubber and plastic in syringes.

Declaration of competing interest

The authors declare that they have no known competing financial interests or personal relationships that could have appeared to influence the work reported in this paper.

CRediT authorship contribution statement

Marco Sorgato: Writing – original draft, Visualization, Investigation, Data curation, Conceptualization. **Kristal Bornillo:** Writing – review & editing, Writing – original draft, Methodology, Conceptualization. **Giovanni Lucchetta:** Writing – review & editing, Writing – original draft, Supervision, Project administration, Funding acquisition, Conceptualization.

Acknowledgments

This project has received funding from the European Union's Horizon 2020 research and innovation program under the Marie Skłodowska-Curie grant agreement No. 956097.

Supplementary materials

Supplementary material associated with this article can be found in the online version at doi:10.1016/j.cirp.2024.04.096.

References

[1] Melo GB, Emerson GG, Dias CS, Morais FB, Lima Filho ADS, Ota S, et al. (2020) Release of Silicone Oil And The Off-Label Use Of Syringes In Ophthalmology. *The British Journal of Ophthalmology* 104/2:291–296.
[2] Thirumangalathu R, Krishnan S, Ricci MS, Brems DN, Randolph TW, Carpenter JF (2009) Silicone Oil- And Agitation-Induced Aggregation Of A Monoclonal Antibody In Aqueous Solution. *Journal of Pharmaceutical Sciences* 98/9:3167–3181.
[3] Yoshino K, Nakamura K, Yamashita A, Abe Y, Iwasaki K, Kanazawa Y, et al. (2014) Functional Evaluation And Characterization Of A Newly Developed Silicone Oil-Free Prefillable Syringe System. *Journal of Pharmaceutical Sciences* 103/5:1520–1528.
[4] Costa HL, Schille J, Rosenkranz A (2022) Tailored Surface Textures To Increase Friction—A Review. *Friction* 10/9:1285–1304.
[5] Niu Y, Pang X, Yue S, Shangguan B, Zhang Y (2021) The Friction And Wear Behavior Of Laser Textured Surfaces In Non-Conformal Contact Under Starved Lubrication. *Wear : an international journal on the science and technology of friction lubrication and wear* : 476.
[6] Schneider J, Braun D, Greiner C (2017) Laser Textured Surfaces For Mixed Lubrication: Influence Of Aspect Ratio, Textured Area And Dimple Arrangement. *Lubricants (Basel, Switzerland)* 5/3.
[7] Lu P, Wood RJK, Gee MG, Wang L, Pfleging W (2018) A Novel Surface Texture Shape for Directional Friction Control. *Tribology Letters* 66/1.
[8] Wang Z, Ye R, Xiang J (2023) The Performance Of Textured Surface In Friction Reducing: A Review. *Tribology International* : 177.
[9] Brinksmeier E, Karpuschewski B, Yan J, Schönemann L (2020) Manufacturing of Multiscale Structured Surfaces. *CIRP Ann* 69/2:717–739.
[10] Berger GR, Gruber DP, Friesenbichler W, Teichert C, Burgsteiner M (2011) Replication of Stochastic and Geometric Micro Structures-Aspects of Visual Appearance. *Int Polym Proc* 26/3:313–322.
[11] Bowden FP, Tabor D (1966) Friction, Lubrication And Wear: A Survey Of Work During The Last Decade. *Br J Appl Sci* 17:1521–1544.
[12] Masato D, Sorgato M, Parenti P, Annoni M, Lucchetta G (2017) Impact of Deep Cores Surface Topography Generated By Micro Milling On The Demolding Force In Micro Injection Molding. *Journal of Materials Processing Technology* 246:211–223.
[13] Zhou J, Qiu Z (2023) The Generation Mechanism of Demolding Force Based On The Mold-Part Interface Contact Mode In Micro-Injection Molding. *Polymer Engineering and Science* 63/3:782–797.
[14] Lucchetta G, Sorgato M, Carmignato S, Savio E (2014) Investigating the Technological Limits of Micro-Injection Molding In Replicating High Aspect Ratio Micro-Structured Surfaces. *CIRP Ann – Manuf Technol* 63/1:521–524.